THE JOURNAL OF PHYSICAL CHEMISTRY B

ARTICLE

pubs.acs.org/JPCB

Dansyl—Naphthalimide Dyads As Molecular Probes: Effect of Spacer Group on Metal Ion Binding Properties

Balaraman H. Shankar and Danaboyina Ramaiah*

Photosciences and Photonics Chemical Sciences and Technology Division, National Institute for Interdisciplinary Science and Technology (NIIST), CSIR, Trivandrum 695 019, India

Supporting Information

ABSTRACT: Interaction of a few dansyl—naphthalimide conjugates **1a**—**e** linked through polymethylene spacer groups with various metal ions was investigated through absorption, fluorescence, NMR, isothermal calorimetric (ITC), and laser flash photolysis techniques. The characteristic feature of these dyads is that they exhibit competing singlet—singlet energy transfer (SSET) and photoinduced electron transfer (PET) processes, both of which decrease with the increase in spacer length. Depending on the spacer group, these dyads interact selectively with divalent Cu^{2+} and Zn^{2+} ions, as compared to other mono- and divalent metal ions. Jobs plot analysis showed that these dyads form 2:3 complexes with Cu^{2+} ions, while 1:1 complexes were observed with Zn^{2+} ions. The association constants for the Zn^{2+} and Cu^{2+} complexes were determined and are found to be in the order 10^3-10^5 M^{-1}. Irrespective of the length of the spacer group, these dyads interestingly act as fluorescence ratiometric molecular probes for Cu^{2+} ions by altering the emission intensity of both dansyl and naphthalimide chromophores. In contrast, only the fluorescence intensity of the naphthalimide chromophore of the lower homologues (n = 1—3) was altered by Zn^{2+} ions. ^{1}H NMR and ITC measurements confirmed the involvement of both sulfonamide and dimethylamine groups in the complexation with Cu^{2+} ions, while only the latter group was involved with Zn^{2+} ions. Laser excitation of the dyads **1a**—**e** showed formation of a transient absorption which can be attributed to the radical cation of the naphthalimide chromophore, whereas only the triplet excited state of the dyads **1a**—**e** was observed in the presence of Cu^{2+} ions. Uniquely, the complexation of **1a**—**e** with Cu^{2+} ions affects both PET and SSET processes, while only the PET process was partially inhibited by Zn^{2+} ions in the lower homologues (n = 1—3) and the higher homologues exhibited negligible changes in their emission properties. Our results demonstrate that the spacer length dependent variations of the photophysical properties of these novel conjugates not only enable the selective detection of Cu^{2+} and Zn^{2+} ions but also aid in discriminating these two biologically important metal ions.

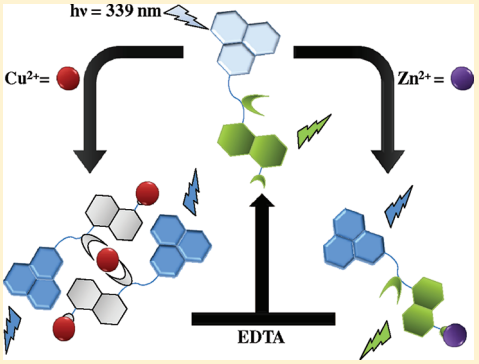

1. INTRODUCTION

The development of chemosensors for essential metal ions,[1] especially copper and zinc ions, has gained increasing importance in recent years because these ions play important roles in living systems and have an extremely toxic impact on the environment.[2] For instance, Cu^{2+} ions are important in maintaining many biological processes, but excess concentrations of these ions can be highly toxic.[3] Cu^{2+} ions are also capable of retarding many enzyme-catalyzed reactions by displacing other metal ions and acting as a cofactor.[3d] Deficiency of copper leads to Menkes disease,[4a] while high levels cause Alzheimer[4b,c] or Wilson disease,[4d] gastrointestinal disorders, and kidney damage. Zn^{2+} ions, on the other hand, play a central role in various biological processes including signal transduction, metabolism of RNA and DNA, gene expression, and numerous other cellular functions.[5] An overdose of Zn^{2+} ions can result in clinical conditions, some of which are similar to those observed with copper deficiency. Due to these reasons, the development of molecular probes that can not only signal the presence of these two metal ions but also differentiate between them is important. Of the various techniques, optoelectronic detection has several advantages and fluorescence-based techniques, in particular, offer high sensitivity.[6]

The most commonly adopted approach in the design of an optical chemosensor is to incorporate a fluorophore (signaling unit) with ion-receptor unit that can bind to various metal ions. The binding of the metal ion with the receptor unit can cause variations in the fluorescence of the fluorophore unit by altering photoinduced electron transfer (PET)[7] or fluorescence resonance energy transfer (FRET)[8] mechanisms, resulting in the sensing of the metal ion. An alternative approach is to employ two different fluorescent units linked via a suitable spacer group characterized by PET and/or singlet—singlet energy-transfer (SSET) mechanisms, so that metal ion binding results in blockade of either one or both of these mechanisms such that a selective fluorescence signaling can be achieved. However, if the

Received: August 17, 2011
Revised: October 8, 2011
Published: October 08, 2011

Chart 1

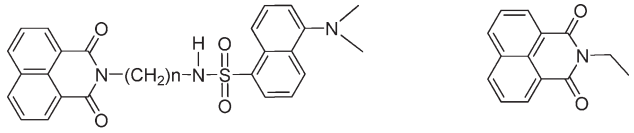

a) n = 2; **b)** n = 3; **c)** n = 4; **d)** n = 6; **e)** n = 8

binding site in the ligand has affinity toward more than one metal ion, such a sensor design can be disadvantageous. Nevertheless, if the binding of one of the metal ions can selectively hinder one relaxation pathway over the other, such a design can be employed to discriminate different metal ions.

Recently, Miranda and co-workers[9a] have reported a few dansyl−naphthalimide dyads linked through a sulfonamide bridging group. The interesting feature of these bichromophoric systems is the presence of two competing relaxation processes: PET from dansyl to the naphthalimide moiety and SSET from the naphthalimide to the dansyl entity. The estimated rates of the PET and SSET indicate that both these relaxation processes decrease with the increase in the length of the spacer group. These dyads contain two potential metal ion binding sites: the sulfonamide as well as the dimethylamine group. It can, therefore, be expected that the interactions of such dyads with different metal ions in principle would alter the photophysical properties and, thus, enable the detection of specific metal ions.

Two binding processes can be envisaged in the dyads **1a**−**e** (Chart 1) in the presence of metal ions: one pertains to the interaction of the metal ion at the dimethylamino group, while the other corresponds to the deprotonation of the sulfonamide bridging unit. Depending on its nature, a metal ion can, thus, partially or completely either perturb PET or hinder the SSET process or inhibit both these processes. In this regard, recently we observed that the higher homologues of these dyads, **1d**−**e**, separated by hexamethylene and octamethylene spacer groups, exhibited selective interactions with Cu^{2+} ions in the micellar medium,[10] wherein the binding of the copper ions at the sulfonamide group blocks the SSET process. Since the rates of the PET and SSET processes vary with the length of the spacer group, it is expected that different metal ions will affect the photophysical properties differently along the dyad series. In the present study, we have systematically investigated the potential of the dyads as selective molecular probes for different metal ions and also the role of the spacer group in the metal ion binding properties. Our results demonstrate that the lower homologues of the dyad series show interactions with both Cu^{2+} and Zn^{2+} ions, while the dyads with longer spacer groups interact only with Cu^{2+} ions and thereby act as sensitive fluorescence ratiometric probes.

2. EXPERIMENTAL SECTION

2.1. Methods. Melting points were determined on a Mel-Temp II melting point apparatus and are uncorrected. Proton NMR data were obtained from a 500 MHz Bruker Avance DPX spectrometer. The electronic absorption spectra were recorded on a Shimadzu UV−vis−NIR spectrophotometer.[11,12] Fluorescence spectra were recorded on a SPEX-Fluorolog F112X spectrofluorimeter. Nanosecond laser flash photolysis experiments were performed by using an Applied Photophysics model LKS-20 laser kinetic spectrometer by using the third harmonic (355 nm) from an OCR-12 Series Quanta Ray Nd:YAG laser. The analyzing and laser beams were fixed at right angles to each other. The laser energy was 64 mJ at 355 nm. Isothermal titration calorimetric titrations were carried out using a Microcal iTC200 microcalorimeter. All data were calculated with Origin ITC data-analysis software.

2.2. General Procedure for the Synthesis of the Dyads 1a−e. Dansyl chloride (5.0 mmol) was added to a stirred solution of the corresponding *N*-(ω-aminoalkyl)-1,8-naphthalimide (4.2 mmol) and triethylamine (5.4 mmol) in dry chloroform (15 mL). The mixture was refluxed for 10 h. After cooling the reaction mixture to room temperature (25 °C), the precipitate obtained was filtered off. The clear filtrate solution was evaporated to dryness under vacuum to give a pale yellow residue, which was chromatographed over silica gel. Elution with a mixture (1:9) of ethyl acetate and hexane gave the dyads **1a**−**e** which were further purified through recrystallization from acetonitrile.

2.3. Calculation of Association Constants. The association between the dyads and Cu^{2+} ions was analyzed using the fluorescence data. The association constants were calculated employing the Benesi−Hildebrand method

$$\frac{1}{(I - I_0)} = \frac{1}{(I - I_{fc})} + \frac{1}{K(I - I_{fc})[Cu^{2+}]^{3/2}} \quad (1)$$

$$\frac{1}{(I - I_0)} = \frac{1}{(I - I_{fc})} + \frac{1}{K(I - I_{fc})[Zn^{2+}]} \quad (2)$$

where K is the association constant, I is the fluorescence intensity of the free dyad, I_0 is the observed fluorescence intensity of the [dyad−M^{2+}] complex, and I_{fc} is the fluorescence intensity at the saturation.

2.4. Isothermal Titration Calorimetry Measurements. ITC experiments were performed at 30 ± 0.1 °C using a MicroCal iTC200 calorimeter. The metal ion titrant (Cu^{2+}, 5.0 mM; Zn^{2+}, 2.5 mM) and dyad solution (0.25 mM, 200 μL) were made from the same acetonitrile solution. The solution in the sample cell was stirred at 1000 rpm by the injection syringe to ensure rapid mixing. Typically, the titrant (2.0 μL) was delivered over 4.0 s with an interval of 3 min between injections to ensure complete equilibration. The data were shown as the baseline-adjusted raw data in the top panel, and the peak-integrated, concentration-normalized heat of reaction versus the molar ratio of metal ions to dyad were presented in the bottom panel. The ITC data was analyzed with the models using the Origin software package (MicroCal LLC ITC program) supplied by MicroCal.[13] A non-linear least-squares algorithm (minimization of χ^2) was used to provide an equilibrium binding model and the best-fit values of the stoichiometry (n), change in enthalpy (ΔH), and binding constant (K).

3. RESULTS

3.1. Synthesis and Photophysical Properties of the Dyads. With a view to prepare bichromophoric dyads of naphthalimide−dansyl linked through varying spacer groups, we have synthesized the dyads **1a**−**e** as reported in the literature.[9,10] The absorption spectra of **1a**−**e** in acetonitrile are shown in Figure 1. These dyads show an absorption maximum at 332 nm with a shoulder at 339 nm. The absorption spectrum of these naphthalimide−dansyl dyads is similar to that of the derivative **2**, implying that

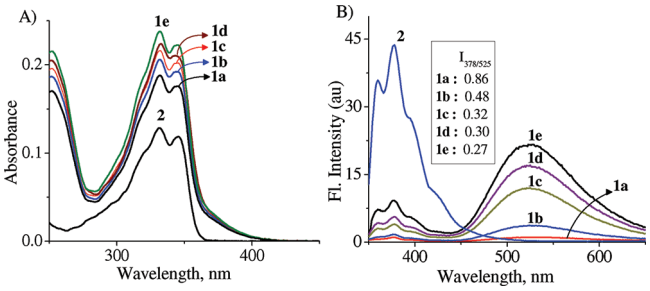

Figure 1. (A) Absorption and (B) emission spectra of the dyads **1a**−**e** (12 μM) and **2** (12 μM) in acetonitrile. λ_{ex} 339 nm. Inset shows the emission intensity ratio $I_{378/525}$.

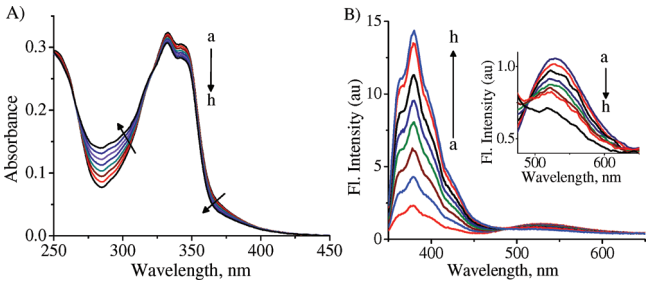

Figure 2. Changes in the (A) absorption and (B) emission spectra of **1a** (6 μM) in acetonitrile with the addition of Cu^{2+} ions [Cu^{2+}] (a) 0 and (h) 12 μM. λ_{ex} = 339 nm. Inset of part B shows the changes in the emission at 525 nm.

there is no ground-state interaction exist between the two choromophores. Emission spectra of these dyads are characterized by two well-spaced maxima at 378 and 525 nm, when excited at 339 nm (where more than 80% of the incident photons are absorbed by the naphthalimide moiety).[9a] The emission at 378 nm can be attributed to the naphthalimide group in the dyads, while the peak at 525 nm is assigned to the dansyl group which arises due to excitation energy transfer from the naphthyl to the dansyl and has been corroborated by the excitation spectral analysis (Figure S1, Supporting Information).

3.2. Metal Ion Binding Properties. Since the dyads **1a**−**e** are characterized by the presence of dual emission bands and possess suitable binding sites for metal ions, it was our interest to investigate the potential of these dyads as fluorescent ratiometric sensors. With this view, we have carried out the interactions of the dyads with various mono and divalent metal ions in acetonitrile. For example, Figure 2A shows the changes in the absorption spectrum of **1a** with the addition of Cu^{2+} ions. With increasing concentration of Cu^{2+} ions, we observed a decrease in the absorption band at 340 nm, with the concomitant increase in the band at 287 nm, with isosbestic points at 265 and 320 nm.

Interestingly, in the emission spectra, the addition of Cu^{2+} ions resulted in the decrease in the SSET mediated dansyl band at 525 nm (Figure 2B). Simultaneously, we could observe the growth of the emission band corresponding to the naphthalimide at 378 nm with an isoemissive point at 485 nm. The addition of 12 μM of Cu^{2+} ions resulted in significant increase in the $I_{378/525}$ value to ca. 20, thereby indicating its potential as a ratiometric sensor for Cu^{2+} ions. The fluorescence changes of the dyad **1a** in the presence of Cu^{2+} ions were analyzed through Jobs and Benesi−Hildebrand plots[14] (Figure S2, Supporting Information),

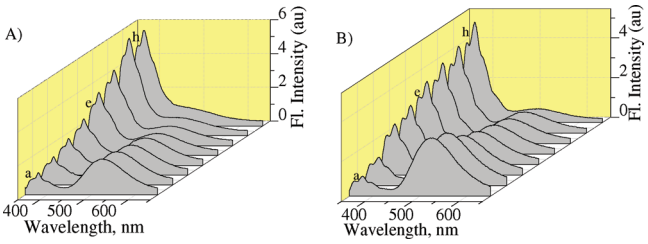

Figure 3. Changes in the emission spectra of (A) **1b** and (B) **1c** (6 μM) in acetonitrile with the addition of Cu^{2+} ions [Cu^{2+}] (a) 0, (e) 6, and (h) 12 μM. λ_{ex} = 339 nm.

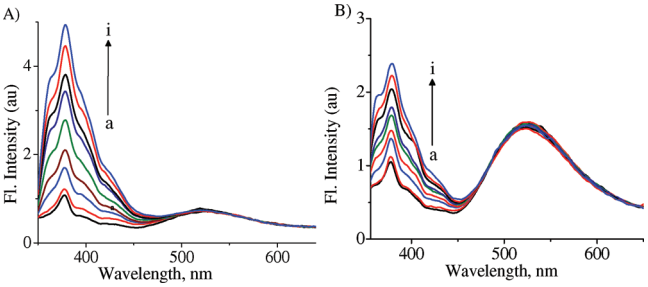

Figure 4. Changes in the emission spectra (A) **1a** (6 μM) and (B) **1b** (6 μM) in acetonitrile with the addition of Zn^{2+} ions. [Zn^{2+}] (a) 0, and (i) 12 μM. λ_{ex} = 339 nm.

which gave a 2:3 stoichiometry for the complexation between **1a** and Cu^{2+} ions, with an overall association constant, $K = (1.19 \pm 0.23) \times 10^5\ M^{-1}$.

Since the dyad **1a** with the dimethylene spacer showed effective interactions with Cu^{2+} ions and since the rates of energy and electron transfer vary with the distance between two chromophores,[15] it was of our interest to study how the variation in the spacer groups affect the interaction of the dansyl−naphthalimide dyads with Cu^{2+} ions (Figure S3, Supporting Information). Figure 3 shows the changes in the fluorescence spectra of dyads **1b** and **1c** with the addition of Cu^{2+} ions. As observed for the dyad **1a**, we could see regular decrease in the emission at 525 nm, with the concomitant increase in the emission corresponding to the naphthalimide at 378 nm (Figure 3A). With increase in the concentration of Cu^{2+} ions, the changes in the emission spectra increased and reached saturation at 1.5 equiv, with a ratiometric change, $I_{378/525}$, of ca. 20-fold. Interestingly, the dyad with tetramethylene spacer, **1c** (Figure 3B), also showed a ratiometric ($I_{378/525}$) change of ca. 20-fold, indicating that the interaction of Cu^{2+} ions with the dyad is not influenced by the length of spacer group. Expectedly, as observed in the case of the dyad **1a**, the Jobs plot analyses of the [dyad−Cu^{2+}] complexation indicated the formation of a 2:3 complex for the dyads **1b**−**e**.

3.3. Selectivity and Reversibility of the Complexation. To investigate the selectivity of the dyads **1a**−**e** for Cu^{2+} ions, we have studied their interactions with other important monovalent and divalent metal ions such as Na^+, Li^+, K^+, Pb^{2+}, Hg^{2+}, Co^{2+}, Fe^{2+}, Cd^{2+}, Mg^{2+}, Ba^{2+}, and Zn^{2+} ions under identical conditions. Notably, all the metal ions, except Zn^{2+} ions, showed negligible interactions toward the various dyads. The addition of Zn^{2+} ions caused negligible changes in the absorption properties of the dyad (Figure S4A, Supporting Information). Interestingly, an

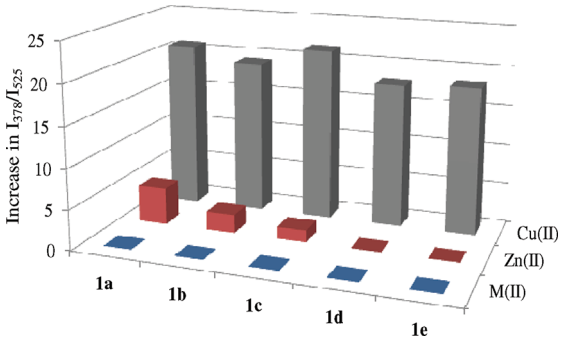

Figure 5. Relative plot showing the increase in I_{378}/I_{525} vs dyads in the presence of various metal ions; Cu^{2+}, Zn^{2+}, and M(II): Pb^{2+}, Hg^{2+}, Co^{2+}, Fe^{2+}, Cd^{2+}, Mg^{2+}, Ba^{2+} ions. λ_{ex} = 339 nm.

enhancement in the fluorescence intensity at 378 nm, corresponding to the naphthalimide was observed in the emission spectra (Figure 4A). Interestingly, the SSET-mediated emission band of the dansyl group at 525 nm showed negligible changes. The changes in the emission of the naphthalimide reached saturation with the addition of 2 equiv of Zn^{2+} ions, with an overall enhancement of ca. 6-fold in the $I_{378/525}$ ratio. Jobs plot analysis of the complexation between the dyad **1a** and Zn^{2+} ions indicated the formation of a 1:1 complex (Figure S2B, Supporting Information) with an association constant of $(7.26 \pm 0.52) \times 10^4$ M^{-1}.

To understand the effect of spacer group, we monitored the interactions with the dyads **1b**−**e** with Zn^{2+} ions. For example, Figure 4B shows the changes in the emission spectrum of the dyad **1b** in the presence of Zn^{2+} ions. As observed in the case of **1a**, the addition of Zn^{2+} ions to the dyad **1b** resulted in the enhancement in the emission band at 378 nm, corresponding to the naphthalimide with no change in the energy-transfer-mediated emission band of the dansyl at 525 nm. However, the extent of enhancement of the naphthalimide emission was lower; ca. 2.3-fold for **1b**, as compared to the ca. 4.6-fold enhancement observed for the dyad **1a**. Similar changes in the emission spectra were observed for the dyad **1c** in the presence of Zn^{2+} ions, albeit with much lower (ca. 1.5 fold) enhancement of the naphthalimide emission band (Figure S4B, Supporting Information). Further increase in the spacer groups to the hexa- and octamethylene, **1d** and **1e**, respectively, caused no significant change in the emission bands of the dyads (Figure 5).

To investigate the reversibility of the complexation of the dyad **1a** with Cu^{2+} and Zn^{2+} ions, ethylenediaminetetraacetic acid (EDTA)[16] was used as the complexing agent (Figure S5, Supporting Information). The dyad, initially, showed dual emission bands with emission maxima at 378 and 525 nm (trace a in Figure S5, Supporting Information). With the addition of Cu^{2+} ions, a significant enhancement in the fluorescence intensity at 378 nm was observed (trace b in Figure S5, Supporting Information). However, when EDTA was added to the solution of the [**1a**−Cu^{2+}] complex, a decrease in the fluorescence intensity corresponding to the naphthalimide moiety was observed. These results demonstrate the reversible binding of Cu^{2+} ions with the dyads (trace c in Figure S5, Supporting Information). Similar observations were made in the case of [dyad−Zn^{2+}] complex with the addition of EDTA.

Figure 5 shows the relative changes in the fluorescence intensity of **1a**−**e** with the addition of different metal ions.

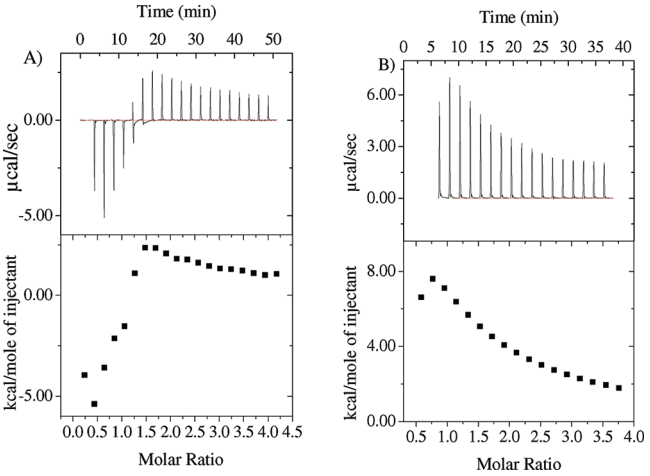

Figure 6. ITC titration of **1a** (0.25 μM) with (A) Cu^{2+} (5.0 μM) and (B) Zn^{2+} (2.5 μM) ions in acetonitrile at 303 K. (Top) Differential power recorded in the experiment. (Bottom) Integration of areas under peaks corresponding to the amount of heat released upon the addition of Cu^{2+} or Zn^{2+} ions to **1a** as a function of the molar ratio ([**1a**]/[M^{2+}]). M = Cu^{2+} or Zn^{2+} ions.

As evident from the figure, the addition of equimolar concentrations of other metal ions caused negligible changes in the fluorescence emission of the various dyads. The interaction of the dyad **1a** toward Cu^{2+} and Zn^{2+} ions can readily be monitored because the fluorescence intensity of **1a** remains unchanged in the presence of the other metal ions, in contrast to the Cu^{2+} and Zn^{2+} ions which cause significant increase in the I_{378}/I_{525} ratio. Noticeably, one can also employ the dyads **1a**−**c** to distinguish between the Cu^{2+} and Zn^{2+} ions, since the Zn^{2+} ions alter only the fluorescence emission intensity at 378 nm.

3.4. Nature of the Complexation. The complexation between the dyads and Cu^{2+} and Zn^{2+} ions was further studied through ^{1}H NMR and isothermal titration calorimetric (ITC) experiments. The ^{1}H NMR spectra of **1a** showed peaks of N−H protons at δ 5.91 ppm, while the six *N*-CH_3 protons appeared as a singlet at δ 2.6 ppm and the methylene protons as a triplet and quartet at δ 4.11 and 3.29 ppm, respectively. The aromatic peaks of the dansyl appeared at δ 6.73, 7.09, 7.30, and 7.95 ppm, whereas the naphthalimide proton signals are observed at δ 7.72 and 8.29 ppm (Figure S6, Supporting Information). Interestingly, the addition of Cu^{2+} ions resulted in significant broadening and the downfield shift of the N−H peak by $\Delta\delta$ = 0.05 ppm, while the peaks corresponding to the *N*-CH_3 protons showed a shift of $\Delta\delta$ = 0.12 ppm. The peaks at δ 7.21 ppm assigned to the aromatic protons of the dansyl broadened with downfield shifts in the range $\Delta\delta$ = 0.03 ppm. In contrast, negligible changes were observed in the napthalimide protons. The association constant values calculated from the Benesi−Hildebrand analysis of δ values corresponding to N−H and *N*-CH_3 were found to be $(4.0 \pm 0.02) \times 10^3$ M^{-1} and $(8.0 \pm 0.1) \times 10^5$ M^{-1}, respectively, and the latter is in agreement with the *K* value obtained for the emission changes. The addition of Zn^{2+} ions to the dyad **1a**, on the other hand, caused less significant changes in the peak at δ 5.6 ppm corresponding to the sulfonamide. As observed in the presence of Cu^{2+} ions, Zn^{2+} ions also caused a shift in the *N*-methyl protons, though to a lesser extent of $\Delta\delta$ = 0.06 ppm (Figure S7, Supporting Information). Further, significant broadening in dansyl aromatic protons could be observed in the ^{1}H NMR spectrum,

Table 1. Binding and Thermodynamic Constants Obtained from Isothermal Titration Calorimetric Experiments of 1a−d with Cu^{2+} and Zn^{2+} Ions[a]

	no. of sites, n	K, M^{-1}	ΔH, cal/mol, 10^4	ΔG^b, cal/mol, 10^3
1a + Cu^{2+}	0.99	$(8.03 \pm 0.05) \times 10^5$ (K_1)	-0.53 ± 0.02	-8.15 ± 0.02
	0.52	$(2.10 \pm 0.14) \times 10^3$ (K_2)	2.88 ± 0.32	-4.58 ± 0.01
1b + Cu^{2+}	0.95	$(7.30 \pm 0.03) \times 10^5$ (K_1)	-0.56 ± 0.01	-8.09 ± 0.01
	0.56	$(2.81 \pm 0.17) \times 10^3$ (K_2)	2.93 ± 0.07	-4.76 ± 0.20
1c + Cu^{2+}	0.98	$(4.06 \pm 0.17) \times 10^5$ (K_1)	-0.54 ± 0.02	-7.74 ± 0.11
	0.55	$(1.01 \pm 0.41) \times 10^3$ (K_2)	1.71 ± 0.45	-4.15 ± 0.02
1d + Cu^{2+}	0.97	$(1.85 \pm 0.81) \times 10^5$ (K_1)	-0.57 ± 0.37	-7.27 ± 0.03
	0.58	$(2.14 \pm 0.96) \times 10^3$ (K_2)	1.18 ± 0.09	-4.60 ± 0.01
1a + Zn^{2+}	1.05	$(1.70 \pm 0.07) \times 10^4$	13.50 ± 0.03	-5.84 ± 0.23
1b + Zn^{2+}	0.98	$(1.51 \pm 0.01) \times 10^4$	5.51 ± 0.11	-5.77 ± 0.61
1c + Zn^{2+}	1.01	$(0.41 \pm 0.01) \times 10^4$	3.73 ± 0.14	-4.99 ± 0.22

[a] Average of more than three independent experiments. [b] Calculated using the equation $\Delta G = -RT \ln K$.

indicating that Zn^{2+} ions interact with the dyads at the dansyl moiety. The association constant calculated from the shift of the N-CH_3 peak is found to be $(6.0 \pm 0.3) \times 10^4$ M^{-1}, which is in agreement with the value obtained from the emission changes.

Isothermal titration calorimetric (ITC) measurements allow the direct determination of the association constant (K), the binding enthalpy (ΔH), and stoichiometry (n, number of binding sites) and provide insights in understanding various interactions. Figure 6 shows the heat evolved per injection plotted against the molar ratio for the calorimetric titration of the dyad **1a** with Cu^{2+} ions. The various thermodynamic parameters involved in the complexation were determined by fitting the ITC data to either one or two independent binding sites model using nonlinear least-squares fitting. As can be seen from the figure, an initial exothermic process was observed with the addition of Cu^{2+} ions, which corresponds to a 1:1 binding process with an association constant of $K_1 = (8.03 \pm 0.05) \times 10^5$ M^{-1}. This is followed by an endothermic event with $K_2 = (2.10 \pm 0.14) \times 10^3$ M^{-1}. The calculated ΔG values obtained for these interactions show that both the binding events are highly feasible, with $\Delta G_1 = -(8.15 \pm 0.02) \times 10^3$ and $\Delta G_2 = -(4.58 \pm 0.01) \times 10^3$ cal/mol. In contrast, the addition of Zn^{2+} ions to a dilute solution of dyad **1a** showed a regular endothermic response at 30 °C as shown in Figure 6. The heat changes, fitted to a one-site binding model, gave an association constant of $(1.70 \pm 0.07) \times 10^4$ M^{-1} with n value of 1.05. The [**1a**−Zn^{2+}] complex showed a free energy change of $-(5.84 \pm 0.23) \times 10^3$ cal mol^{-1}. Similar observations were made with the other dyads, **1b**−**d** (Figure S8, Supporting Information), and the thermodynamic parameters for the interactions are tabulated in Table 1.

3.5. Laser Flash Photolysis Studies. Since the dyads involve an electron-transfer process from the dansyl moiety to the naphthalimide, the binding of the metal ions at the N-CH_3 of the dansyl group is expected to inhibit this process. With this view, we have studied the excited-state properties of the dyads in the presence and absence of the metal ions and the transient intermediates have been characterized by nanosecond laser flash photolysis of the dyads. Excitation of **1a** by 355 nm pulse gave the transient spectrum with absorption maximum at 410 nm. On the basis of literature reports,[17] we assign this peak to the naphthalimide radical anion formed as a result of PET from dansyl moiety to the naphthalimide chromophore (trace a in Figure S9, Supporting Information).

With the addition of Cu^{2+} ions to a solution of the dyad **1a**, the peak corresponding to the naphthalimide radical anion disappeared with the concomitant appearance of new peaks at 360, 440, and 470 nm. The transient absorption is readily quenched by dissolved oxygen, suggesting that the transient absorption could be due to the triplet excited state of the dyad. This transient absorption spectra obtained for the [dyad−Cu^{2+}] complex is characteristic of the T_1−T_n absorption of the naphthalimide in the triplet excited state (trace b in Figure S9, Supporting Information).[17] Interestingly, the formation of the triplet excited state of the naphthalimide has been observed for all the dyads, irrespective of the spacer group, in the presence of Cu^{2+} ions. However, in the presence of Zn^{2+} ions we could observe the transient absorption of the naphthalimide radical anion, albeit with lower intensity, indicating thereby the partial inhibition of the photoinduced electron-transfer process (trace c in Figure S9, Supporting Information).

4. DISCUSSION

The excited states of the dyads **1a**−**e** are characterized by the mechanisms of SSET and PET processes. These processes can be easily visualized from the emission spectra of the dyads with dual bands at 378 and 525 nm, which correspond to naphthalimide and SSET-mediated dansyl emission, respectively. It is noteworthy that both these phenomena vary with the spacer, the dyad with the longest spacer group having the lowest rate of SSET/PET.[18] Nevertheless, all these dyads fall within the critical distance for the energy transfer of 14.4 Å.[19]

The dyads **1a**−**e** showed selective interactions with Cu^{2+} and Zn^{2+} ions when compared to other mono- and divalent metal ions. With the addition of Cu^{2+} ions, the formation of a new band could be observed in the absorption spectra at 287 nm with a decrease in the absorption maximum at 340 nm. This new absorption band can be attributed to the deprotonation of the sulfonamide group by the metal ion, which results in the blue-shifted absorption of the dansyl chromophore.[20] Notably, the deprotonation of the sulfonamide bridging group precludes the energy-transfer process (SSET). As a result, inhibition of the energy-transfer-mediated emission of the dansyl moiety is observed, which enables the ratiometric monitoring of the presence of Cu^{2+} ions.

In the ^1H NMR spectra, considerable broadening and downfield shift can be observed in the peaks corresponding to

Scheme 1. Structure of the Complexes Formed by 1a with Cu^{2+} and Zn^{2+} Ions

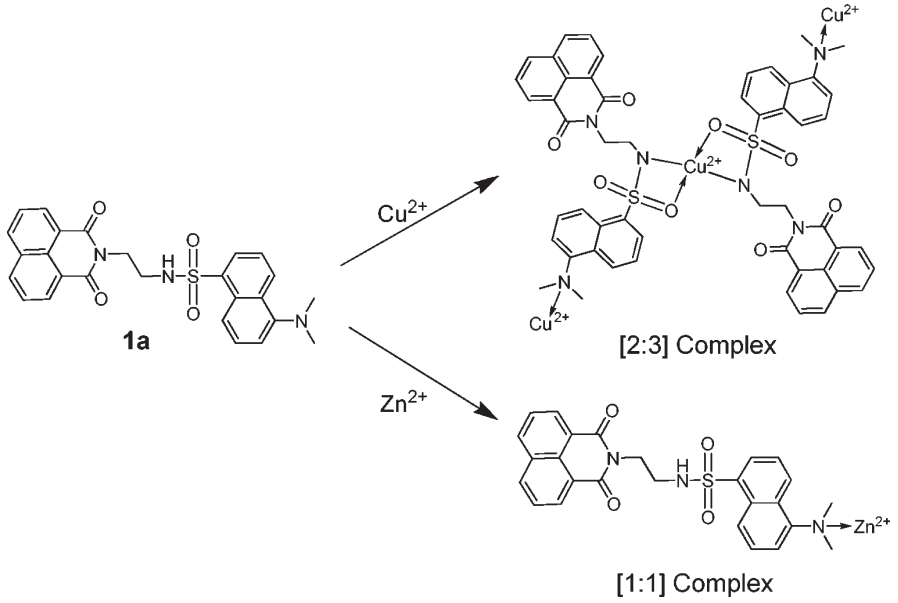

sulfonamide and *N*-methyl protons, upon interaction with Cu^{2+} ions. This indicates that both the sulfonamide and the *N*-methyl groups act as potential sites for interaction with Cu^{2+} ions (Scheme 1). Such an interaction is also consistent with the formation of the 2:3 [dyad−Cu^{2+}] complex indicated by the Jobs plot analysis. This is, further, confirmed by the ITC experiments, wherein we could observe two distinct binding events—an exothermic and an endothermic process in the presence of Cu^{2+} ions. The exothermic process with an *n* value of ca. 1.0 corresponds to the formation of a 1:1 complex between Cu^{2+} ions and the dyads and can be attributed to the binding at the *N,N*-dimethylamine group of the dansyl moiety. The association constant for this binding interaction, and hence the associated free energy change, decreases considerably with the increasing spacer group [$(8.03 \pm 0.05) \times 10^5\ M^{-1}$ for **1a** ($n = 2$) and $(1.85 \pm 0.81) \times 10^5\ M^{-1}$ for **1d** ($n = 6$)]. Nevertheless, the enthalpy change for this process remains more or less constant for all the dyads. The second binding event as seen from the ITC experiments is an enthalpy-driven process which could be attributed to the deprotonation of the sulfonamide group. The *n* value observed for this process, ca. 0.5, pertains to the formation of a 2:1 complex with respect to the dyad. As expected, this deprotonation process is not significantly affected by the spacer length; negligible difference is observed in the ΔG values across the dyad series. However, both these processes are favorable as indicated by the negative ΔG values (Table 1). Thus, the overall binding stoichiometry is two ligands to three Cu^{2+} ions, which is in agreement with the observations made with the analysis of Jobs plot and photophysical changes.

Interestingly, the higher value of the association constants, calculated from the ^1H NMR and ITC changes, for the interaction of the Cu^{2+} ions at the *N,N*-dimethylamine group suggests a much stronger affinity for this site when compared to the binding at the sulfonamide group. This can be readily understood if we consider the high reduction potential of copper ions in acetonitrile.[21] Moreover, the unusual redox chemistry of Cu^{2+} ions (reduction potential of Cu^{2+} ions in acetonitrile is about 1 V versus SCE, which is much positive than in water)[21b] implies the absence of the $N(CH_3)_2-Cu^{2+}$ interaction in the aqueous medium, as observed previously for the dyad with the octamethylene spacer groups, wherein Cu^{2+} ions perturbed only the SSET processs without affecting the PET process in the micellar medium.[10]

On the basis of these observations, we propose that the interaction of Cu^{2+} ions at the *N,N*-dimethylamine group prevents PET process from the dansyl to the naphthalimide moeity, while the deprotonation of the sulfonamide group disrupts the SSET process; the important aspect being the complete perturbation of both these process throughout the dyad series in the presence of Cu^{2+} ions. This is evidenced in the nanosecond laser flash photolysis studies wherein we observed the complete disappearance of the transient absorption corresponding to the radical anion of naphthalimide in the presence of Cu^{2+} ions. Under these conditions, we observed only the triplet excited state of the naphthalimide moiety due to the breakage of both PET as well as SSET processes. Since copper ions cause the complete disruption of both the process, the ratio of I_{378}/I_{525} remained the same for all the dyads as manifested by the spacer-length-independent ratiometric signaling of Cu^{2+} ions.

On the other hand, the interaction of Zn^{2+} ions with the dyads causes negligible changes in the absorption spectra revealing the nonalteration of the electronic levels of the dyads. Interestingly, Zn^{2+} ions significantly enhance the emission of the naphthalimide at 378 nm, with negligible changes at the SSET mediated dansyl emission. Jobs plot analysis indicated the formation of a 1:1 complex as represented in Scheme 1, with the Zn^{2+} ions interacting at the dimethylamino group alone. This interaction is indicated by the shift in the corresponding proton peak at δ 2.8 ppm. The lower value of the association constant ($6 \times 10^4\ M^{-1}$) obtained for this interaction, as compared to that of Cu^{2+} ions ($7.6 \times 10^5\ M^{-1}$), indicates the less strong interactions of Zn^{2+} ions toward the dyads. This is also clear from the ITC experiments which, further, confirmed the formation of a 1:1 complex with association constants of the order of $10^4\ M^{-1}$. Notably, a

significant decrease in the K values was observed with increasing spacer length. This trend is also reflected in the photophysical studies, wherein the extent of the fluorescence enhancement of the naphthalimide chromophore (378 nm) was found to decrease considerably from **1a** to **1e**.

More importantly, the interaction of Zn^{2+} ions with the dyads at the dimethylamino group shows negligble influence on SSET reaction in these dyads, but partially affects the PET process. This is, in turn, reflected in the negligible changes at the energy-transfer-mediated dansyl emission during the fluorescence titrations. The observation of the transient absorption of the napthalimide radical anion even in the presence of Zn^{2+} ions indicates that the electron-transfer process is only partially inhibited, rather than a complete inhibition as observed in the [**1a**−Cu^{2+}] complex. The negligible emission changes observed for the higher homologues of the dyad series in the presence of Zn^{2+} ions as compared to the lower series is in tune with the observation of the lower values of the rate of PET for the former over the latter series.

5. CONCLUSIONS

We have systematically investigated the effect of the spacer group and metal ion binding on a few dansyl−naphthalimide dyads characterized by opposing PET and SSET processes. All these dyads, irrespective of the spacer group, can act as selective ratiometric fluorescence probes for Cu^{2+} ions, wherein both the processes PET and SSET are inhibited. In contrast, these dyads exhibited spacer length dependent interactions with Zn^{2+} ions, with the lower homologues exhibiting the maximum affinity. The uniqueness of this study is that, although these dyads interact effectively and selectively with both Cu^{2+} and Zn^{2+} ions as compared to other mono- and divalent metal ions, due to their contrary redox character, these two metal ions affect the photophysical processes in the dyads differently. As a result, these dyads are capable of differentiating Cu^{2+} ions even in the presence of Zn^{2+} ions and signal the event through the ratiometric fluorescence emission.

■ ASSOCIATED CONTENT

Supporting Information. Figures S1−S9 showing absorption, fluorescence, ^{1}H NMR, and transient absorption spectra and isothermal calorimetry titration data. This material is available free of charge via the Internet at http://pubs.acs.org.

■ AUTHOR INFORMATION

Corresponding Author

*Tel.: (+91) 471 2515362. Fax: (+91) 471 2490186, (+91) 471 2491712. E-mail: rama@niist.res.in, d_ramaiah@rediffmail.com.

■ ACKNOWLEDGMENT

This work was supported by the Department of Science and Technology (DST), Government of India, and the National Institute for Interdisciplinary Science and Technology (CSIR-NIIST), Trivandrum. This is Contribution No. PPG-318 from NIIST, Trivandrum.

■ REFERENCES

(1) (a) de Silva, A. P.; Gunaratne, H. Q. N.; Gunnlaugsson, T.; Huxley, A. J. M.; McCoy, C. P.; Rademacher, J. T.; Rice, T. E. *Chem. Rev.* **1997**, *97*, 1515–1566. (b) Valeur, B.; Leray, I. *Coord. Chem. Rev.* **2000**, *205*, 3–40. (c) Fabbrizzi, L.; Licchelli, M.; Mancin, F.; Pizzeghello, M.; Rabaioli, G.; Taglietti, A.; Tecilla, P.; Tonellato, U. *Chem.—Eur. J.* **2002**, *8*, 94–101. (d) Jyothish, K.; Avirah, R. R.; Ramaiah, D. *Org. Lett.* **2006**, *8*, 111–114. (e) de Silva, A. P.; Uchiyama, S. *Nat. Nanotechnol.* **2007**, *2*, 399–410. (f) Shiraishi, Y.; Ishizumi, K.; Nishimura, G.; Hirai, T. *J. Phys. Chem. B* **2007**, *111*, 8812–8822.

(2) (a) Ros-Lis, J. V.; Garcia, B.; Jimenez, D.; Martinez-Manez, R.; Sancenon, F.; Soto, J.; Gonzalvo, F.; Valldecabres, M. C. *J. Am. Chem. Soc.* **2004**, *126*, 4064–4065. (b) Gokel, G. W.; Leevy, W. M.; Weber, M. E. *Chem. Rev.* **2004**, *104*, 2723–2750. (c) Montvydiene, D.; Marciulioniene, D. *Environ.Toxicol.* **2004**, *19*, 351–358.

(3) (a) Kramer, R. *Angew. Chem., Int. Ed.* **1998**, *37*, 772–773. (b) Torreggiani, A.; Domènech, J.; Orihuela, R.; Ferreri, C.; Atrian, S.; Capdevila, M.; Chatgilialoglu, C. *Chem.—Eur. J.* **2009**, *15*, 6015–6024. (c) Koval, I. A.; Gamez, P.; Belle, C.; Selmeczi, K.; Reedijk, J. *Chem. Soc. Rev.* **2006**, *35*, 814–840.

(4) (a) Vulpe, C.; Levinson, B.; Whitney, S.; Packman, S.; Gitschier, J. *Nat. Genet.* **1993**, *3*, 7–13. (b) Barnham, K. J.; Masters, C. L.; Bush, A. I. *Nat. Rev. Drug Discovery* **2004**, *3*, 205–214. (c) Jiao, Y.; Yang, P. *J. Phys. Chem. B* **2007**, *111*, 7646–7655. (d) Rodriguez-Granillo, A.; Crespo, A.; Wittung-Stafshede, P. *J.Phys. Chem. B 114*, 1836− 1848 *J. Phys. Chem. B* **2010**, *114*, 1836–1848.

(5) (a) Berg, J. M.; Shi, Y. *Science* **1996**, *271*, 1081–1085. (b) Zhang, L.; Clark, R. J.; Zhu, L. *Chem.—Eur. J.* **2008**, *14*, 2894–2903. (c) Outtenand, C. E.; O'Halloran, T. V. *Science* **2001**, *292*, 2488–2492. (d) Jiang, P.; Guo, Z. *Coord. Chem. Rev.* **2004**, *248*, 205–229. (e) McMahon, R. J.; Cousins, R. J. *Proc. Natl. Acad. Sci. U.S.A.* **1998**, *95*, 4841–4846. (f) Dudev, T.; Lim, C. *J. Phys. Chem. B* **2001**, *105*, 10709–10714.

(6) (a) Métivier, R.; Leray, I.; Valeur, B. *Chem.—Eur. J.* **2004**, *10*, 4480–4490. (b) Constable, E. C.; Martinez-Manez, R.; Cargill Thompson, A. M. W.; Walker, J. V. J. *J. Chem. Soc., Dalton Trans.* **1994**, 1585–1594. (c) Jisha, V. S.; Arun, K. T.; Hariharan, M.; Ramaiah, D. *J. Am. Chem. Soc.* **2006**, *128*, 6024–6025. (d) Neelakandan, P. P.; Hariharan, M.; Ramaiah, D. *J. Am. Chem. Soc.* **2006**, *128*, 11334–11335. (e) Arun, K. T.; Ramaiah, D. *J. Phys. Chem. A* **2005**, *109*, 5571–5578. (f) Weerasinghe, A. J.; Schmiesing, C.; Varaganti, S.; Ramakrishna, G.; Sinn, E. *J. Phys. Chem. B* **2010**, *114*, 9413–9419. (g) Xu, Z.; Yoon, J.; Spring, D. R. *Chem. Soc. Rev.* **2010**, *39*, 1996–2066.

(7) (a) Fabbrizzi, L.; Poggi, A. *Chem. Soc. Rev.* **1995**, *24*, 197–202. (b) Kim, J. S.; Quang, D. T. *Chem. Rev.* **2007**, *107*, 3780–3799. (c) Wasielewski, M. R. *Acc. Chem. Res.* **2009**, *42*, 1910–1921. (d) Hanaoka, K.; Muramatsu, Y.; Urano, Y.; Terai, T.; Nagano, T. *Chem.—Eur. J.* **2010**, *16*, 568–572.(e) *Photoinduced Electron Transfer*; Fox, M. A., Channon, M., Eds.; Elsevier: Amsterdam, 1988. (f) Lu, X.; Zhu, W.; Xie, Y.; Li, X.; Gao, Y.; Li, F.; Tian, H. *Chem.—Eur. J.* **2010**, *16*, 8355–8364.

(8) (a) Kim, H. J.; Hong, J.; Hong, A.; Ham, S.; Lee, J. H.; Kim, J. S. *Org. Lett.* **2008**, *10*, 1963–1966. (b) Arduini, M.; Felluga, F.; Mancin, F.; Rossi, P.; Tecilla, P.; Tonellato, U.; Valentinuzzi, N. *Chem. Commun.* **2003**, 1606–1607. (c) Van Dongen, E. M. W. M.; Dekkers, L. M.; Spijker, K.; Meijer, E. W.; Klomp, L. W. J.; Merkx, M. *J. Am. Chem. Soc.* **2006**, *128*, 10754–10762. (d) Ma, C.; Zeng, F.; Huang, L.; Wu, S. *J. Phys. Chem. B* **2011**, *115*, 874–882. (e) Sanju, K. S.; Neelakandan, P. P.; Ramaiah, D. *Chem. Commun.* **2011**, *47*, 1288–1290.

(9) (a) Abad, S.; Kluciar, M.; Miranda, M. A.; Pischel, U. *J. Org. Chem.* **2005**, *70*, 10565–10568. (b) Lee, M. H.; Kim, H. J.; Yoon, S.; Park, N.; Kim, J. S. *Org. Lett.* **2008**, *10*, 213–216. (c) Battistuzzi, G. G.; Grandi, G.; Menabue, L.; Pellacani, G. C.; Sola, M. *J. Chem. Soc., Dalton Trans.* **1985**, 2363–2368.

(10) Jisha, V. S.; Thomas, A. J.; Ramaiah, D. *J. Org. Chem.* **2009**, *74*, 6667–6673.

(11) (a) Joseph, J.; Eldho, N. V.; Ramaiah, D. *J. Phys. Chem. B* **2003**, *107*, 4444–4450. (b) Sajimon, M. C.; Ramaiah, D.; Suresh, C. H.; Adam, W.; Lewis, F. D.; George, M. V. *J. Am. Chem. Soc.* **2007**, *129*, 9439–9445. (c) Kuruvilla, E.; Ramaiah, D. *J. Phys. Chem. B* **2007**, *111*, 6549–6556. (d) Arun, K. T.; Jayaram, D. T.; Avirah, R. R.; Ramaiah, D. *J. Phys. Chem. B* **2011**, *115*, 7122–7128. (e) Neelakandan, P. P.; Nandajan, P. C.; Subymol, B.; Ramaiah, D. *Org. Biol. Chem.* **2011**, *9*, 1021–1029.

(12) (a) Neelakandan, P. P.; Ramaiah, D. *Angew. Chem., Int. Ed.* **2008**, *47*, 8407–8411. (b) Jisha, V. S.; Arun, K. T.; Hariharan, M.; Ramaiah., D. *J. Phys. Chem. B* **2010**, *114*, 5912–5919. (c) Kuruvilla, E.; Joseph, J.; Ramaiah, D. *J. Phys. Chem. B* **2005**, *109*, 21997–22002.

(13) (a) Zhang, Y.; Akilesh, S.; Wilcox, D. E. *Inorg. Chem.* **2000**, *39*, 3057–3064. (b) Grossoehme, N. E.; Akilesh, S.; Guerinot, M. L.; Wilcox, D. E. *Inorg. Chem.* **2006**, *45*, 8500–8508. (c) Grossoehme, N. E; Mulrooney, S. B; Hausinger, R. P.; Wilcox, D. E. *Biochemistry* **2007**, *46*, 10506–10516.

(14) (a) Benesi, H. A.; Hildebrand, J. H. *J. Am. Chem. Soc.* **1949**, *71*, 2703–2707. (b) Yannis, L. L. *J. Phys. Chem. B* **1997**, *101*, 4863–4866. (c) Kim, H. J.; Hong, J.; Hong, A.; Ham, S.; Lee, J. H.; Kim, J. S. *Org. Lett.* **2008**, *10*, 1963–1966. (d) Avirah, R. R.; Jyothish, K.; Ramaiah, D. *J. Org. Chem.* **2008**, *73*, 274–279.

(15) (a) Vadim, V. K. *J. Phys. Chem.* **1992**, *96*, 2609–2613. (b) Joseph, J.; Eldho, N. V.; Ramaiah, D. *Chem.—Eur. J.* **2003**, *9*, 5926–5935. (c) Neuteboom, E. E.; Van Hal, P. A.; Janssen, R. A. J. *Chem.—Eur. J.* **2004**, *10*, 3907–3918. (d) Tsoi, W. C.; O'Neill, M.; Aldred, M. P.; Kitney, S. P.; Vlachos, P.; Kelly, S. M. *Chem. Mater.* **2007**, *19*, 5475–5484. (e) Murata, S.; Tachiya, M. *J. Phys. Chem.* **1996**, *100*, 4064–4070. (f) Langhals, H.; Obermeier, A.; Floredo, Y.; Zanelli, A.; Flamigni, L. *Chem.—Eur. J.* **2009**, *15*, 12733–12744.

(16) (a) Arunkumar, E.; Chithra, P.; Ajayaghosh, A. *J. Am. Chem. Soc.* **2004**, *126*, 6590–6598. (b) Zaitoun, M. A.; Lin, C. T. *J. Phys. Chem. B* **1997**, *101*, 1857–1860.

(17) (a) Wintgens, V.; Valat, P.; Kossanyi, J.; Biczok, L.; Demeter, A.; Berces, T. *J. Chem. Soc., Faraday Trans.* **1994**, *90*, 411–421. (b) Jones, G.; Kumar, S. *J. Photochem. Photobiol. A: Chem* **2003**, *160*, 139–149.

(18) (a) Portela, C. F.; Brunckova, J.; Richards, J. L.; Schöllhorn, B.; Iamamoto, Y.; Magde, D.; Traylor, T. G.; Perrin, C. L. *J. Phys. Chem. A* **1999**, *103*, 10540–10552. (b) Pettersson, K.; Kilså, K.; Mårtensson, J.; Albinsson, B. *J. Am. Chem. Soc.* **2004**, *126*, 6710–6719. (c) Kuragaki, M.; Sisido, M. *J. Phys. Chem.* **1996**, *100*, 16019–16025.

(19) Speiser, S. *Chem. Rev.* **1996**, *96*, 1953–1976.

(20) (a) Koike, T.; Watanabe, T.; Aoki, S.; Kimura, E.; Shiro, M. *J. Am. Chem. Soc.* **1996**, *118*, 12696–12703. (b) Deo, S.; Godwin, H. A. *J. Am. Chem. Soc.* **2000**, *122*, 174–175. (c) Kim, J. S.; Quang, D. T. *Chem. Rev.* **2007**, *107*, 3780–3799.

(21) (a) Inamo, M.; Kumagai, H.; Harada, U.; Itoh, S.; Iwatsuki, S.; Ishihara, K.; Takagi, H. D. *Dalton Trans.* **2004**, 1703–1707. (b) Sreenath, K.; Suneesh, C. V.; Ratheesh Kumar, V. K.; Gopidas, K. R. *J. Org. Chem.* **2008**, *73*, 3245–3251. (c) Senthilvelan, A.; Ho, I.-T.; Chang, K.-C.; Lee, G.-H.; Liu, Y.-H.; Chung, W.-S. *Chem.—Eur. J.* **2009**, *15*, 6152–6160.